ORIGINAL ARTICLE

Enhanced PAPR reduction in DCO-OFDM using multi-point constellations and DPSO optimization

Volkan Aydin[1] · Gokce Hacioglu[2]

Abstract

DC-biased optical OFDM (DCO-OFDM) is a commonly used method of OFDM in visible light communication (VLC). Unfortunately, VLC systems that use OFDM often experience a high peak-to-average power ratio (PAPR). To address this issue, this study proposes a novel method called the multi-point constellation method (MPC) to reduce PAPR in DCO-OFDM. The MPC method involves adding extra alternative constellation points around the existing points and using the discrete particle swarm optimization (DPSO) algorithm to select the constellation points with the lowest PAPR. The proposed MPC method is also combined with selective mapping (SLM), a well-known PAPR reduction technique in the literature. Simulation results show that the proposed MPC method outperforms the SLM method in reducing PAPR in 4-QAM and 16-QAM modulations when used in combination with SLM. Furthermore, increasing the number of iterations and particles in the DPSO algorithm improves the PAPR reduction performance of the proposed method even further.

Keywords Visible light communications · VLC · PAPR · OFDM · DPSO · Multi-point constellation

1 Introduction

The use of LEDs in ambient lighting, the limited bandwidth, and the need for high-speed communication has led to the development of visible light communication (VLC) [1, 2]. However, the location of the LED armatures on the ceiling, the position of the receiver on the floor, and the data rate can cause Inter-Symbol Interference (ISI) in VLC [3]. To mitigate ISI, Orthogonal Frequency Division Multiplexing (OFDM), which is commonly used in radio frequency (RF) systems, can be utilized in VLC [4]. In the intensity modulated direct detection (IM/DD) method, which is frequently used in VLC, the transmitted symbols must be real-valued and positive [5]. To address this, OFDM can be employed in IM/DD systems by utilizing Hermitian symmetry [6].

One of the major issues with the OFDM method is the high peak-to-average power ratio (PAPR) at the output. In VLC systems, high PAPR values can result in damage to LEDs and nonlinear clipping distortion [4]. However, limiting the transmitted signal power to avoid clipping distortion can lead to inefficient use of LEDs [7]. Therefore, an effective PAPR reduction technique is needed at the transmitter [8, 9]. Various PAPR reduction techniques have been proposed for OFDM-based VLC systems [10–12].

The tone injection (TI) method is one of several PAPR reduction methods that have been adapted for VLC systems [13–15]. Other methods include active constellation extension (ACE) [16], tone reservation [17, 18], nonlinear companding and clipping [19], and the exponential nonlinear companding algorithm [20]. In addition, a pilot carrier-assisted PAPR reduction technique [21] and a selective mapping (SLM) method where side information (SI) is removed [22, 23] have also been proposed for VLC systems.

Additional alternatives are introduced for the original constellation points in TI method. However, unlike our proposed method, the alternatives for an original

✉ Gokce Hacioglu
gokcehacioglu@ktu.edu.tr

Volkan Aydin
volkan_aydn2000@ktu.edu.tr

1   Surmene Abdullah Kanca Vocational School of Higher Education, Karadeniz Technical University, Camburnu Surmene, 61530 Trabzon, Turkey

2   Department of Electrical and Electronics Engineering, Karadeniz Technical University, KTU Kanuni Kampusu, 61080 Trabzon, Turkey

constellation point in the TI method might not be the closest to that original constellation point among other original constellation points. As a result, the tone injection method can cause a considerable increase in power [24]. Furthermore, implementing the TI method requires a higher processing workload for the receiver's detection process. The ACE method involves moving the original M-QAM constellation points and expanding the constellation. However, the receiver does not need to know all possible extended constellation points because a moved version of an original constellation point is closest to the original constellation point among other original constellation points, as proposed in this paper. However, the ACE method cannot extend all the constellation points; it can only be applied to exterior constellation points [25]. In the TR method, some subcarriers are used not for carrying information but for reducing the PAPR. The subcarriers used for PAPR reduction are called reserved tones. The number of reserved tones, in other words, the amount of side information, can be quite significant [18]. The clipping method can cause a significant decrease in the bit error rate performance [26]. Clipping also causes out-of-band interference. When companding techniques are employed to reduce the out-of-band interference in clipping, the bit error rate (BER) performance is also improved [27]. Pilot-assisted PAPR reduction scheme transmits a block full of pilot symbols after a certain number of OFDM blocks (such as 4). However, the side information required for SLM (Selected Mapping) is lower, and the PAPR performance is better than the pilot-assisted PAPR reduction scheme [21].

This study proposes a unique PAPR reduction method for VLC systems. The proposed method adds a certain number of new constellation points around each constellation point, increasing the number of constellation points while allowing the receiver to detect the data sent using the original constellation points. The discrete particle swarm optimization (DPSO) algorithm selects constellation points from among the alternatives to give the lowest PAPR for each subcarrier. The proposed extended constellation points are then used in conjunction with selective mapping (SLM) to further reduce PAPR, at the cost of sending side information to the receiver. The performance of the proposed method in terms of both PAPR and BER is examined and shown to perform significantly well.

The paper is organized as follows: Sect. 2 describes the proposed multipoint constellation method, while Sect. 2.1 outlines the utilization of DPSO for the proposed method. The performance results of the proposed method are presented in Sect. 3. Finally, the conclusions are discussed in Sect. 4.

Notations: Matrices are denoted by bold uppercase letters, and vectors are denoted by bold lowercase letters. The

$[.]^\mathrm{T}$ notation represents the transpose operation. The $E[.]$ notation represents the expectation operator.

2 The proposed method

The proposed multi-point constellation (MPC) scheme is a modulation scheme where incoming bits are mapped by M-QAM constellations, and L alternatives are added to each of M constellation points. These alternatives are generated by expanding the original constellation points in Δ steps in a rectangular or circular area, controlled by a parameter r. The minimum distance between the alternatives of different constellation points is denoted by $d_{\mathrm{out,min}}$. If $d_{\mathrm{in,max}} < d_{\mathrm{out,min}}$, the receiver can detect the original symbols using the original constellation points. Figures 1 and 2 show the 4-QAM extended constellations obtained if constellation points are expanded within the rectangular and circular area.

The proposed scheme can be combined with selective mapping (SLM) to further reduce the PAPR. In the SLM technique, the N symbols obtained by mapping are multiplied by the weighting coefficients selected from the rows or columns of a weight matrix. However, due to Hermitian symmetry, only $N/2 - 1$ distinct symbols can be carried by N subcarriers in VLC systems. Therefore, $N/2 - 1$ distinct weighting coefficients should be selected from the rows or columns of the matrix. The **s** array containing $N/2 - 1$ symbols to be transmitted is shown in Eq. 1. The symbols $s_1, s_2, ..., s_j; (j = N/2 - 1)$ are mapped according to M-QAM modulation with respect to incoming binary data, while $k_1, k_2, ..., k_j \in [1, 2, ..., L]$ show the alternate point number determined independently for each symbol to be transmitted.

If SLM is used, $m_{i,1}, m_{i,2}, ... m_{i,j}$ represent $N/2 - 1$ elements in row i of the SLM weighting matrix. On the other hand, if SLM is not used, $m_{i,1}, m_{i,2}, ... m_{i,j}$ are all equal to 1.

$$\mathbf{s} = \begin{bmatrix} m_{i,1}s_{1,k_1} & m_{i,2}s_{1,k_2} & \dots & m_{i,j}s_{j,k_j} \end{bmatrix} \tag{1}$$

In Eq. 2, $\mathbf{s_t}$ represents the time-domain signal after applying Hermitian symmetry and inverse fast Fourier transform (IFFT). The operation $\mathbf{F}^H$ represents the conjugate transpose of the Fourier transformation matrix, and flip denotes the left-to-right flipping of the elements of an array. The $*$ operator represents the complex conjugate. The resulting signal is a time-domain representation of the frequency-domain signal **s**, which has been extended to include the Hermitian symmetry.

$$\mathbf{s_t} = \mathbf{F}^H \times \begin{bmatrix} 0 & \mathbf{s} & 0 & \mathrm{flip}(\mathbf{s}^*) \end{bmatrix}^\mathrm{T} \tag{2}$$

The values of $k_1, k_2, ..., k_j$ and i can be determined as follows to obtain lower peak-to-average power ratio.

4-QAM Constellation points and the alternatives
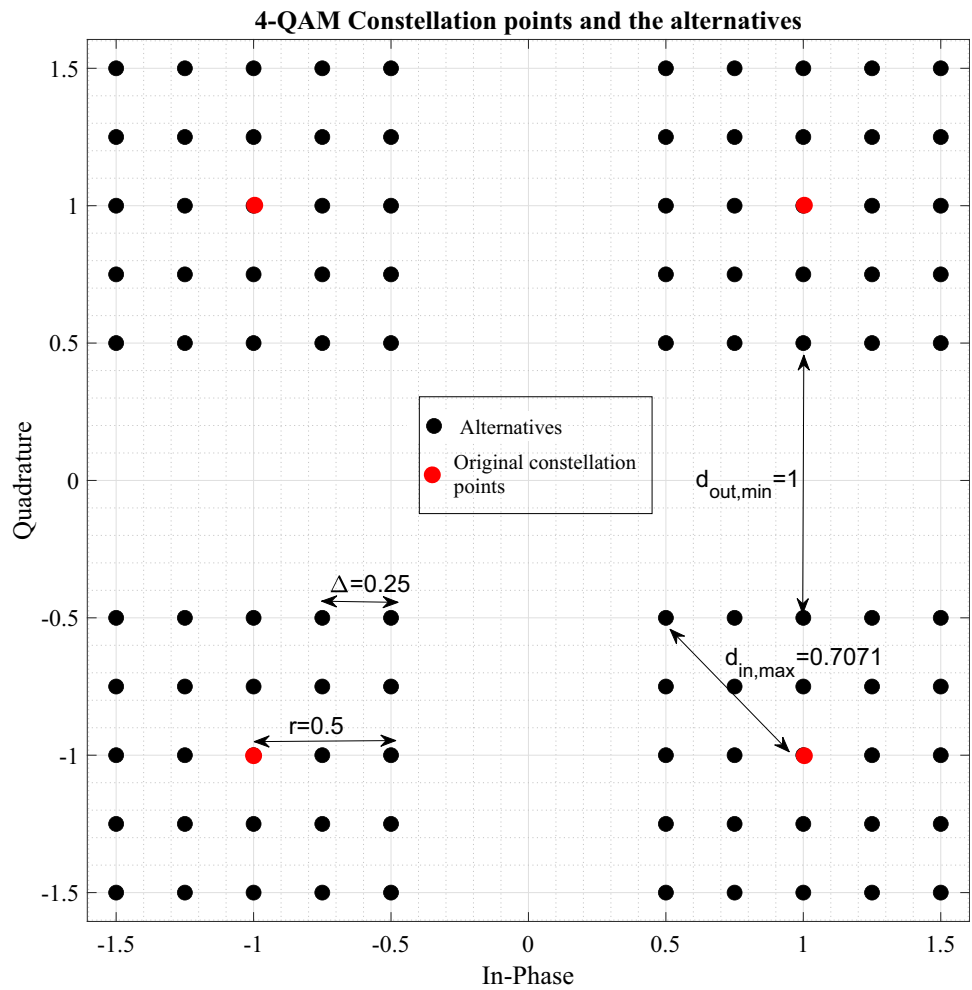
$$\text{argmin}_{k_1, k_2, \ldots, k_j, i} \left(\frac{\max(\mathbf{s_t} \odot \mathbf{s_t})}{E[\mathbf{s_t} \odot \mathbf{s_t}]} \right) \qquad (3)$$

The system model is presented in Fig. 3. The green (MPC), red (MPC+SLM), and blue (SLM) boxes represent the PAPR reduction methods compared in this study. If the MPC method is used, no side information is transmitted to the receiver. However, in the SLM and SLM+MPC methods, side information is transmitted to inform receiver about the index number of the row of the weight matrix.

## 2.1 The proposed DPSO solution

In 1995, Kennedy and Eberhart developed Particle Swarm Optimization (PSO) [28]. Later, in 1998, Shi and Eberhart introduced a variant of PSO called Discrete PSO (DPSO) [29, 30]. PSO is frequently employed to tackle problems through virtual agents known as "particles." Each particle possesses a position and a velocity, both determined by vectors representing potential solutions. The position signifies the particle's location within the solution space,

while the velocity denotes the rate of positional change. Particles are updated by progressing toward their best-known solution and incorporating the best solutions of other particles within the group. This process continues until all particles converge to a local minimum or a specified tolerance level. The DPSO algorithm has demonstrated its effectiveness over PSO in addressing discrete optimization problems, exhibiting superior speed and accuracy [31].

For the resolution of discrete optimization problems, both the Genetic Algorithm (GA) and the DPSO algorithm can be applied. However, research indicates that DPSO achieves convergence with fewer iterations compared to GA [32]. While GA excels in terms of converging toward global optima, PSO gains preference in scenarios involving computational workload [33, 34]. In fact, recent studies have concentrated on the utilization of DPSO for solving discrete optimization problems [31, 35, 36].

Since the problem in Eq. 3 is a NP-Hard problem, it was decided that it would be appropriate to solve it using the DPSO algorithm. In the proposed method, DPSO is used to

Fig. 2 Circular extended constellations for 4-QAM
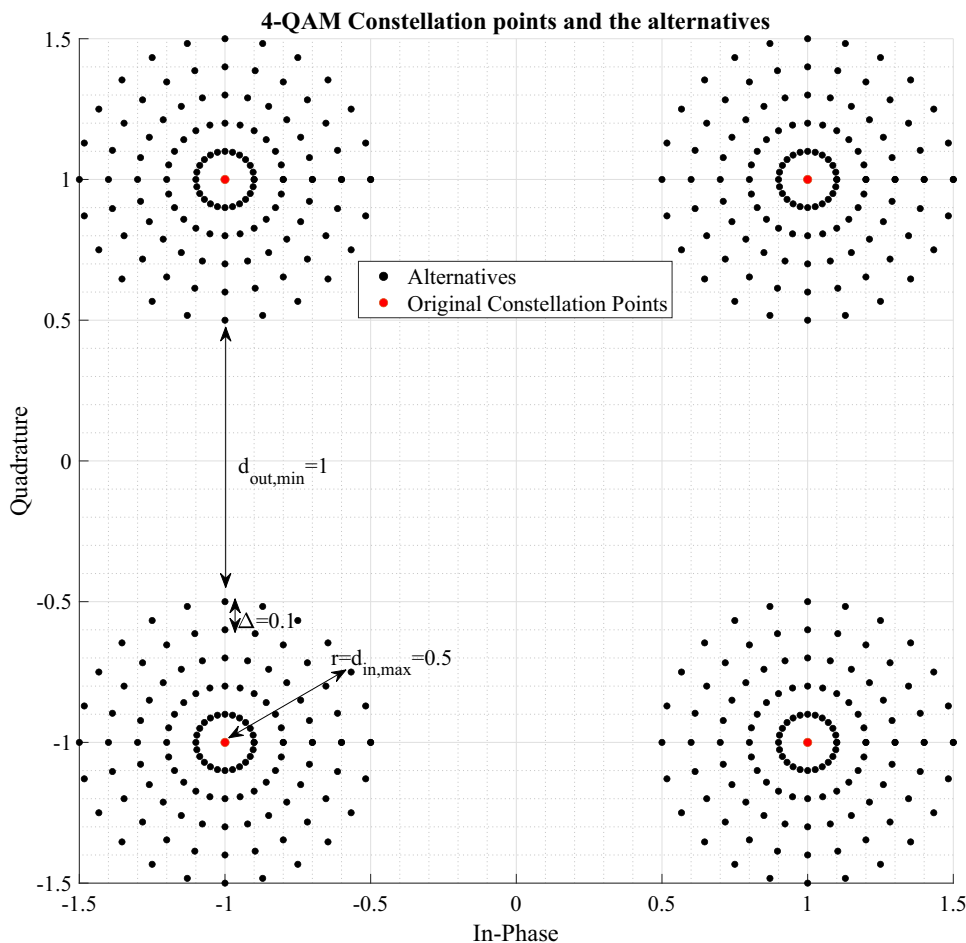
select one of the L alternatives for each symbol to be transmitted. DPSO is also used to select one of the rows of the weighting matrix when SLM and the proposed MPC method are used together. It is assumed that P particles are used in the DPSO algorithm. For each of the total P particles, the constellation alternative number $(k_1, k_2, \ldots, k_j)$ and the row number i of the SLM weight coefficients matrix are determined by DPSO. N-point IFFT is taken and P different PAPR values are found for each of the particles. After the DPSO algorithm calculates the IFFT for each of the P particles, it determines the smallest PAPR value that all the particles have achieved so far and stores the corresponding parameters included in a vector consisting of binary values as the global best (gb). The lowest PAPR value achieved by a particular particle (e.g., mth particle) is determined, and the corresponding binary vector is stored as the personal best (pb_m) of that particle.

After K iterations of the DPSO algorithm, the proposed method obtains the alternative constellation numbers and the row number of the SLM weighting matrix from the global best vector gb, which provides the lowest PAPR value. As a result, the proposed method performs a total of $P \times K$, N-point IFFTs. The alternative numbers

$k_1, k_2, \ldots, k_j$ and the row number i are represented by $A = \lceil \log_2(L) \rceil$ and $B = \lceil \log_2(N) \rceil$ bits, respectively. The position vector x_m of the mth particle contains $A + B$ bits, while the velocity vector v_m contains $A + B$ elements between 0 and 1. After each iteration of the DPSO, the position and velocity vectors of the particles are updated according to Eqs. (4) and (5), where $v_{m,k}$ and $x_{m,k}$ denote the kth element of the velocity and position vectors of the mth particle. The constants c_1 and c_2 are used in the calculations, and r_1 and r_2 are vectors with $A + B$ random valued elements. The number of rows in the weight matrix can be greater than the number of transmitted symbols, but only $\frac{N}{2} - 1$ weight coefficients are taken from a specified ith row.

$$v_m = v_m + c_1 r_1 \odot (pb_m - x_m) + c_2 r_2 \odot (gb - x_m) \qquad (4)$$

$$s(v_{m,k}) = \frac{1}{1 + e^{-v_{m,k}}} ; x_{m,k} = \begin{cases} 1 & \text{if } \mathrm{rand}() \leq s(v_{m,k}) \\ 0 & \text{otherwise} \end{cases}$$

$$(5)$$

Algorithm 1 Algorithm of Using DPSO for MPC+SLM

1: **function gb** $=\text{MPCSLM}(M, N, P, K, r, \Delta, [s_1, s_2, ..., s_j])$

2: $\quad L = \left(2 \times \left(\frac{r}{\Delta}\right) + 1\right)^2 \quad$ ▷ Number of total constellation points for rectangular extension

3: $\quad N_2 = \frac{N}{2} - 1 \quad$ ▷ Number of active symbols to be transmitted

4: $\quad$ Generate constellation points as depicted in Fig. 1 and Fig. 2, and store them in the matrix $\mathbf{C_M}$ $(L \times M)$

5: $\quad$ Generate a weighting matrix, such as the Hadamard matrix, denoted as W_H $(N \times N)$

6: $\quad A = \lceil \log_2(L) \rceil \quad$ ▷ Number of bits for constellation points

7: $\quad B = \lceil \log_2(N_2) \rceil \quad$ ▷ Number of bits for the row number i of the Hadamard matrix

8: $\quad$ Generate a binary random array **gb** $(1 \times N_2 \times (A + B)) \quad$ ▷ This will be the outcome after the iterations of DPSO

9: $\quad gbval = 1000 \quad$ ▷ An initially assigned large PAPR value to the global best

10: $\quad$ Create P particles, each containing a randomly assigned binary matrix $\mathbf{x_m}$ of size $(1 \times N_2 \times (A + B))$ (Equation 4.)

11: $\quad$ Assign to each of the P particles the binary random array $\mathbf{pb_m}$ $(1 \times N_2 \times (A + B))$ (Equation 4.)

12: $\quad pbval_m = 1000 \quad$ ▷ An initially assigned large PAPR value to the personal best values

13: $\quad$ Randomly assign the velocity matrix $\mathbf{v_m}$ $(1 \times N_2 \times (A + B))$ to each particle, with uniformly distributed values between 0 and 1

14: $\quad$ **for** $mmk = 1$ to K **do**

15: $\quad\quad$ **for** $m = 1$ to P **do**

16: $\quad\quad\quad$ Get the $\mathbf{x_m}$ for particle m

17: $\quad\quad\quad$ Obtain $(k_1, k_2, ..., k_j \in [0, 1, ..., L - 1])$ and i from $\mathbf{x_m}$

18: $\quad\quad\quad$ Obtain $\mathbf{s}$ and $\mathbf{s_t}$ Using Equations 1 and 2

19: $\quad\quad\quad$ Calculate the PAPR value of particle m: $PAPR_m = \left(\frac{\max(\mathbf{s_t} \odot \mathbf{s_t})}{E[\mathbf{s_t} \odot \mathbf{s_t}]}\right)$, (Equation 3)

20: $\quad\quad\quad$ **if** $PAPR_m < pbval_m$ **then**

21: $\quad\quad\quad\quad pbval_m = PAPR_m$

22: $\quad\quad\quad\quad \mathbf{pb_m} = \mathbf{x_m}$

23: $\quad\quad\quad$ **end if**

24: $\quad\quad\quad$ **if** $PAPR_m < gbval$ **then**

25: $\quad\quad\quad\quad gbval = PAPR_m$

26: $\quad\quad\quad\quad \mathbf{gb} = \mathbf{x_m}$

27: $\quad\quad\quad$ **end if**

28: $\quad\quad$ **end for**

29: $\quad\quad$ **for** $m = 1$ to P **do**

30: $\quad\quad\quad$ Update $\mathbf{v_m}$ and $\mathbf{x_m}$ using Equations 4 and 5

31: $\quad\quad$ **end for**

32: $\quad$ **end for**

33: **end function**

When only the SLM method is used, all the rows of the weight matrix are evaluated to find the row number i that provides the lowest PAPR. Then, the resulting vector $\mathbf{s_t}$ is

Fig. 3 System model
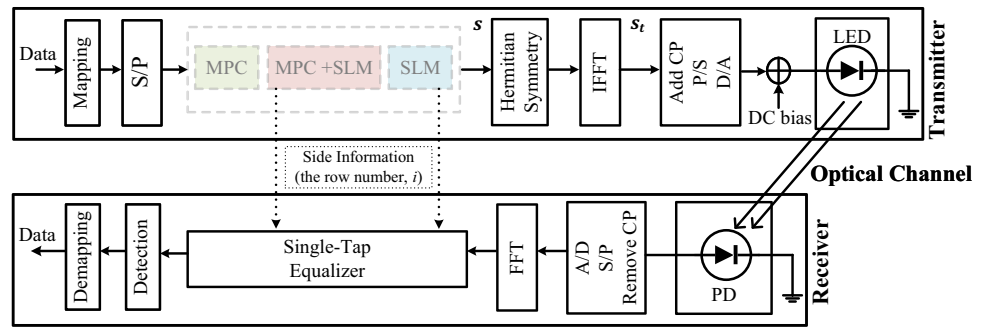
obtained. It is assumed that a cyclic prefix (CP) was added before transmission at the transmitter and removed at the receiver. The resulting vector $\mathbf{r_t}$ is obtained at the receiver. In the case of the MPC method, $\mathbf{r_t}$ is directly used to detect $\mathbf{s_t}$. However, in the SLM and SLM+MPC methods, side information is used to detect $\mathbf{s_t}$ from $\mathbf{r_t}$. The pseudocode for the proposed method is illustrated in Algorithm 1.

$$\mathbf{r_t} = \mathbf{H s_t} + \mathbf{n_t} \tag{6}$$

The N samples received are the elements of $\mathbf{r}_t$, which are corrupted by Additive White Gaussian Noise (AWGN) represented by the vector $\mathbf{n}_t$. The $\mathbf{H}$ matrix represents a circulant channel matrix of size $N \times N$. At the receiver, the FFT is applied to $\mathbf{r}_t$ to convert the multi-tap channel to a single-tap channel as follows.

$$\mathbf{\Lambda}^{-1} \times \mathbf{F} \times \mathbf{r_t} = \begin{bmatrix} 0 & \tilde{\mathbf{s}} & 0 & \text{flip}(\tilde{\mathbf{s}}^*) \end{bmatrix}^T \tag{7}$$

Here, $\tilde{\mathbf{s}}$ denotes the noisy version of the vector $\mathbf{s}$ in Eq. 1. The matrix $\mathbf{\Lambda}$ is a diagonal matrix, and the circulant channel matrix $\mathbf{H}$ can be expressed as $\mathbf{H} = \mathbf{F}^H \times \mathbf{\Lambda} \times \mathbf{F}$. If the proposed MPC method and SLM are not used together, the receiver would not need to know any side information, and the received symbols can be detected as shown below:

$$\widehat{s_k} = c_j = \text{argmin}_j \left| \tilde{s_k} - c_j \right| \tag{8}$$

The jth original constellation point, which is not extended, is represented by c_j, and the detected symbol at index k is denoted by $\widehat{s_k}$. Additionally, the kth element of $\tilde{\mathbf{s}}$ is represented by $\tilde{s_k}$. If the SLM method is used in conjunction with the proposed MPC method, the detection process would be as follows:

$$\widehat{s_k} = c_j = \text{argmin}_j \left| \tilde{s_k} - m_{i,k} c_j \right| \tag{9}$$

To apply the SLM method in conjunction with the proposed MPC method, the receiver needs to know the kth weighting coefficient of the ith row of the weight matrix. One way to achieve this is by sending the row number i to the receiver as side information, assuming that the receiver is already aware of the specific weight matrix used (e.g., Hadamard matrix, as in our simulations).

3 Simulation results

The proposed MPC method has been applied to an indoor VLC system. The complementary cumulative distribution function (CCDF), which describes the probability that a random variable exceeds a certain threshold, was used to measure the PAPR performance. In addition, the bit error rate (BER) performance was analyzed since a PAPR reduction method should not reduce the BER performance below an acceptable level.

$$\begin{aligned} \text{CCDF} &= \text{Pr}\left(10 \log_{10}\left(\frac{\max(\mathbf{s_t} \odot \mathbf{s_t})}{E[\mathbf{s_t} \odot \mathbf{s_t}]} \right) > y_0 \right) \\ &= \text{Pr}(\text{PAPR}_{\text{dB}} > y_0) \end{aligned} \tag{10}$$

CCDF refers to the probability that the Peak-to-Average Power Ratio (PAPR) in dB exceeds a specified threshold value y_0. In the case of the Discrete Particle Swarm Optimization (DPSO) algorithm, the number of iterations and particles is represented by K and P, respectively. The parameters c_1 and c_2 in Eq. 4 are set to 2. The modulation technique used for M-ary Quadrature Amplitude Modulation (M-QAM) mapping involves M values of 4 and 16. Furthermore, the weight matrix consists of an $N \times N$ Hadamard matrix, and the SLM and MPC methods are applied individually and in combination for N values of 64 and 128 subcarriers. Regardless of whether the MPC method is used in conjunction with SLM, DPSO necessitates $K \times P$ IFFT evaluations.

Figures 4 and 5 show that rectangular extended constellations offer the best PAPR performance for $M = 4$, $M = 16$, and $N = 128$. While the MPC method alone cannot exceed the PAPR performance of the SLM method, combining the proposed MPC method with SLM can achieve better PAPR performance. In SLM, 128 IFFT operations are required for $N = 128$ as all rows are evaluated to identify the row with the lowest PAPR of the 128×128 weight matrix. However, the combined SLM and MPC method requires $K \times P = 10 \times 10 = 100$ IFFT operations to achieve better PAPR performance than SLM alone for both $M = 4$ and $M = 16$. The proposed method can provide a gain of $1.46dB$ more than SLM with only 247
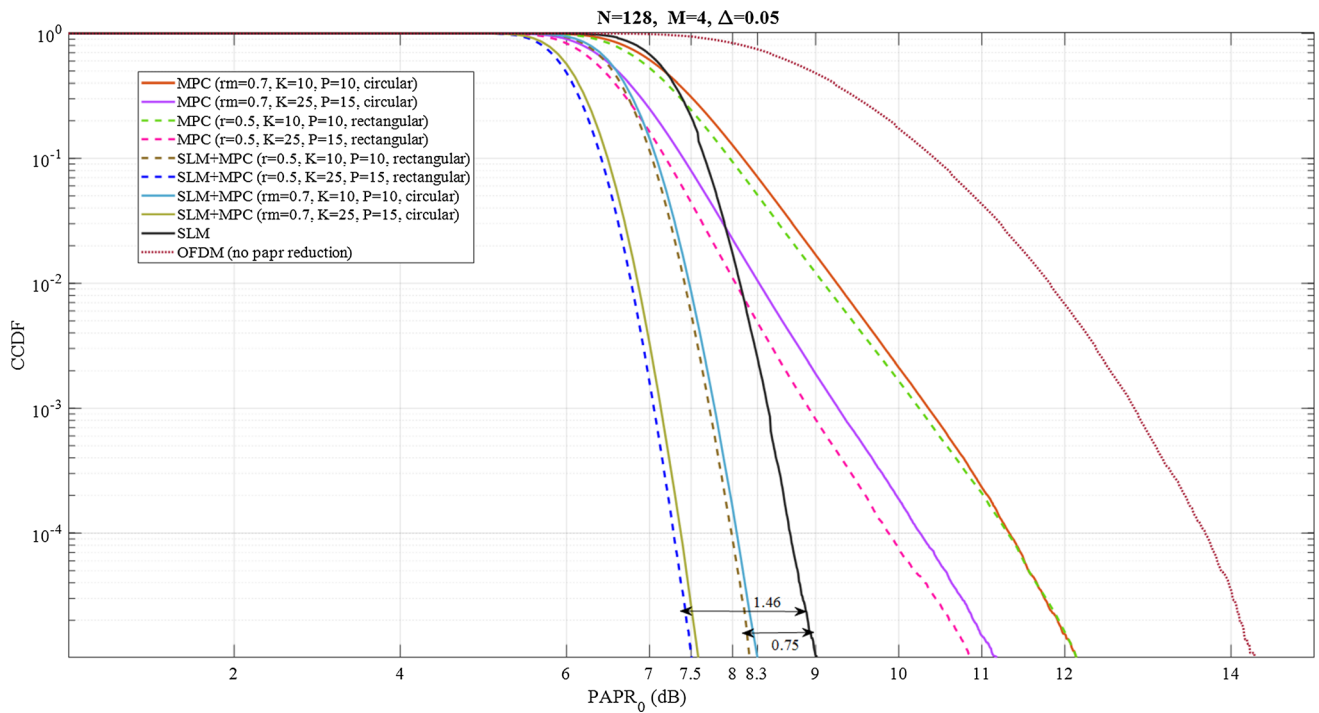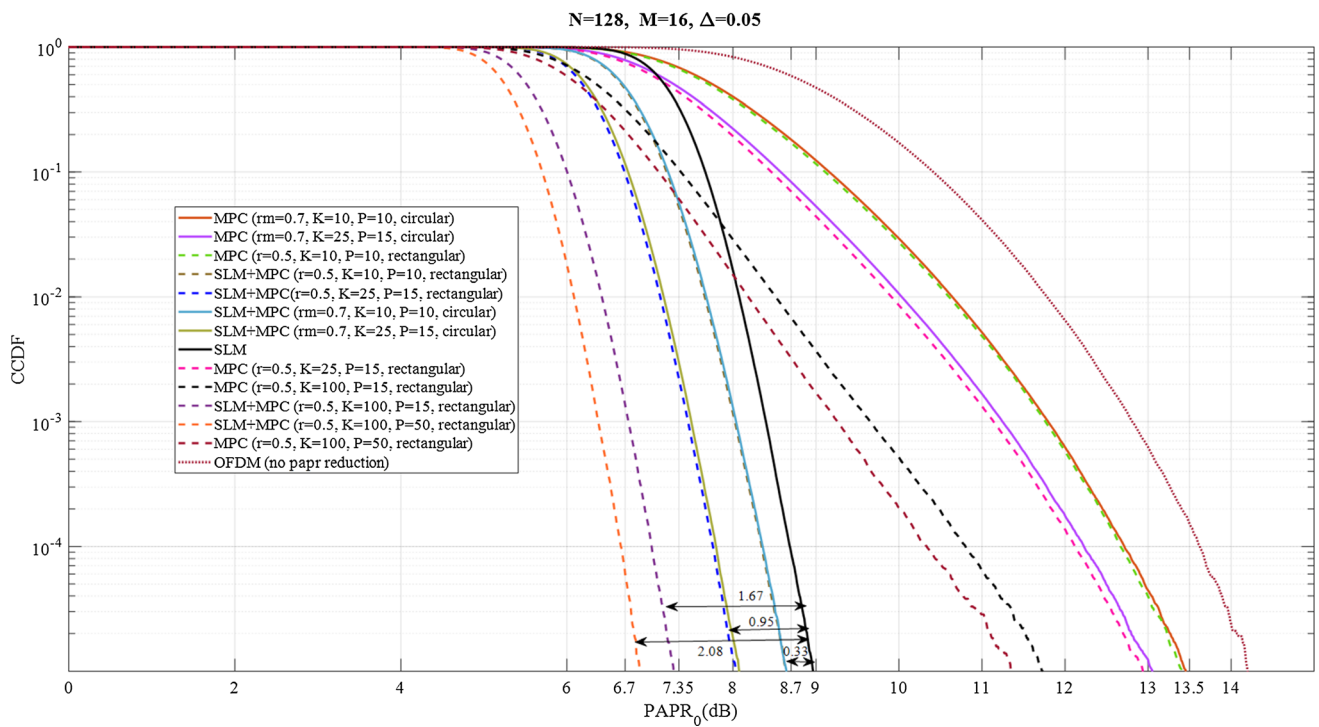
Fig. 4 4-QAM PAPR performances

Fig. 5 16-QAM PAPR performances

more IFFT computational cost, as shown in Fig. 4. However, for $128 - 100 = 28$ fewer IFFT calculations, the proposed method provides a gain of $0.75dB$ more than SLM. Figure 5 further examines the PAPR performance of

the proposed method for $M = 16$, demonstrating that increasing the number of particles and iterations leads to greater PAPR reduction gains. When SLM and MPC are

Table 1 T test results

	N = 128, 4-QAM			N = 128, 16-QAM		
	T	s.d	d.f	T	s.d	d.f
SLM and SLM+MPC (K=10, P=10)	3079	0.5424	7,178,728	2365	0.5743	7,178,728
SLM and MPC (K=10, P=10)	208.8	0.7704	7,178,728	-1717	1.0357	7,178,728
OFDM and SLM+MPC(K=10, P=10)	2215	1.1164	999,999	2077	1.1309	999,999
OFDM and MPC (K=10, P=10)	1534	1.2444	999,999	829	1.421	999,999
SLM and SLM+MPC (K=25, P=15)	6163	0.5170	7,178,728	4733	0.5517	7,178,728
SLM and MPC (K=25, P=15)	2717	0.669	7,178,728	− 410	0.9587	7,178,728
OFDM and SLM+MPC(K=25, P=15)	2748	1.1055	999,999	2516	1.1195	999,999
OFDM and MPC (K=25, P=15)	2137	1.1826	999,999	1240	1.3669	999,999
SLM+MPC (K=25, P=15) and SLM+MPC (K=10, P=10)	− 3045	0.4979	7,178,728	− 2200	0.5696	7,178,728

combined, the PAPR reduction gain compared to SLM can reach up to 2.08dB.

We conducted an analysis of the Peak-to-Average Power Ratio (PAPR) results using a T test to determine whether the proposed methods (MPC, SLM+MPC) yield significantly different outcomes compared to both the unmodified OFDM and SLM methods. The T test also helped us determine if there were any significant differences in the PAPR results based on changes in the iteration and population sizes of the DPSO algorithm. The test results are displayed in Table 1, including the T score, standard deviation (s.d), and degrees of freedom (d.f). The hypothesis test result (H) consistently equals one and the p value for each case has been determined to be zero. When $H = 1$, it means that the mean of the difference between two samples (such as SLM and SLM+MPC) is not zero. The large T score values in Table 1 indicate that the compared methods are significantly different. Moreover, the T test involves at least one million samples (d.f + 1). The p value of zero suggests that the results were not obtained by chance.

It is considered that selecting appropriate values for the iteration number (K) and particle number (P) in DPSO can result in both lower PAPR and reduced computational load. Table 2 displays the SNR levels necessary for the MPC, SLM+MPC, and SLM techniques to attain a BER (Bit Error Rate) value of 3.8×10^{-3}. This BER value represents the accepted threshold for forward error correction (FEC) when using $N = 128$. The BER performance of the MPC and SLM+MPC methods is not affected by the K and P values of the DPSO algorithm. When using the proposed MPC method, optimal BER performance is achieved by using a rectangular extension of the constellation points.

The results demonstrate that the FEC limit BER value can be achieved at an acceptable SNR value by using rectangular expanded constellation points and the SLM method together, while optimizing for the lowest PAPR value with DPSO. However, it should be noted that the clipping values outside the dynamic range of the LEDs, defined by the threshold (V_{th}) and saturation (V_{sat}) voltage levels, were not considered when calculating the results presented in Table 2. To ensure that the values obtained at the output of the IFFT fall within the dynamic range of the

Table 2 The FEC limit performances

Modulation					
4-QAM			16-QAM		
	SNR for FEC limit (3.8×10^{-3})			SNR for FEC limit (3.8×10^{-3})	
SLM	10.7 dB			17.3 dB	
	Circular extension	Rectangular extension (dB)		Circular extension (dB)	Rectangular extension (dB)
MPC	17.5	14.55		23.9	20.6
SLM+MPC	17.5	14.55		23.9	20.6

LED for illumination, they must be multiplied by a scaling factor (α) [37]. Additionally, a DC bias value (V_{dc}) should be added to the IFFT output to be transmitted. The scaled and DC added version of the IFFT output to be transmitted is denoted as ($\mathbf{s}_{t,scaled}$).

$$\mathbf{s}_{t,scaled} = \alpha \mathbf{s}_t + V_{dc} \qquad (11)$$

A small scaling factor indicates a low power of the information-carrying part of the signal. In this study, the Cree Xlamp XB-H datasheet values of $V_{sat} = 3.15$ V and $V_{th} = 2.65$ V were used. A DC bias value of 3 V was used as V_{dc} in the simulations. With the parameters $M = 16$, $N = 128$, $K = 100$, and $P = 25$, a scaling factor α was calculated for each OFDM block to ensure that the LED was in the dynamic region and to prevent clipping. The power of the scaled IFFT output is denoted as p_{signal} and has values of -21.4833 dB, -23.0209 dB, and -23.8146 dB for SLM+MPC, SLM, and without any PAPR reduction, respectively, for the mean of 20,000 OFDM blocks. The SLM+MPC method provided 1.5376 dB more signal power than the SLM method, which could result in a higher SNR value for the same receiver.

4 Conclusion

The multi-point constellation (MPC) method was proposed in this study to achieve lower PAPR in the DCO-OFDM method. The proposed method can reduce the PAPR value by 7 dB compared to DCO-OFDM for 128 carriers and 16-QAM modulation. Discrete particle swarm optimization is used in the proposed method to find the alternative constellation points. When the iterations and number of particles are increased, the proposed method performs a better PAPR reduction at the cost of a high processing load; the minimum number of iterations and particles was chosen as 10, and an approximate 6 dB gain was obtained compared to DCO-OFDM. Although the methods proposed were applied to a VLC DCO-OFDM system, they can also be used with most of the OFDM systems proposed for optical and RF communications. To reduce processing load, the proposed method may be used when the PAPR value of the original constellation points is above a certain threshold value. Future studies will experimentally implement the proposed method. Additionally, other meta-heuristic methods besides DPSO will be tested, and the achieved performances will be compared, considering the computational workloads. When the proposed method and SLM are used together, weight coefficients are selected from the rows of the Hadamard matrix. These weight coefficients are multiplied with alternative constellation points, and the resulting new sample values undergo IFFT.

In the future, a PAPR reduction method will be investigated that involves randomly generating a certain number of matrices, including the proposed MPC method, and selecting one of these matrices to minimize the PAPR.

Declarations

Conflict of interest The authors have no conflicts of interest to declare that are relevant to the content of this article.

References

1. Chowdhury MZ, Hossan MT, Islam A, Jang YM (2018) A comparative survey of optical wireless technologies: Architectures and applications. IEEE Access 6:9819–9840
2. Feng L, Hu RQ, Wang J, Xu P, Qian Y (2016) Applying VLC in 5G networks: architectures and key technologies. IEEE Netw 30(6):77–83
3. Singh ML, Singh M, Gill HS, Kaur S (2021) Quantitative analysis of different led lamp configurations in indoor VLC system. Int J Commun Syst 34(14):4916
4. Armstrong J, Schmidt BJ (2008) Comparison of asymmetrically clipped optical OFDM and DC-biased optical OFDM in AWGN. IEEE Commun Lett 12(5):343–345
5. Pathak PH, Feng X, Hu P, Mohapatra P (2015) Visible light communication, networking, and sensing: a survey, potential and challenges. IEEE Commun Surv Tutor 17(4):2047–2077
6. Zhang X, Babar Z, Petropoulos P, Haas H, Hanzo L (2021) The evolution of optical OFDM. IEEE Commun Surv Tutor 23:1430–1457
7. Elgala H, Mesleh R, Haas H (2009) Non-linearity effects and predistortion in optical OFDM wireless transmission using LEDs. Int J Ultra Wideband Commun Syst 1(2):143–150
8. Han SH, Lee JH (2005) An overview of peak-to-average power ratio reduction techniques for multicarrier transmission. IEEE Wirel Commun 12(2):56–65
9. Hasan MM (2014) PAPR reduction in OFDM systems based on autoregressive filtering. Circuits Syst Signal Process 33(5):1637–1654

10. Sharifi AA (2019) PAPR reduction of optical OFDM signals in visible light communications. ICT Express 5(3):202–205

11. Wang J, Xu Y, Ling X, Zhang R, Ding Z, Zhao C (2016) PAPR analysis for OFDM visible light communication. Opt Express 24(24):27457–27474

12. Alrakah HT, Gutema TZ, Sinanovic S, Popoola WO (2022) PAPR reduction in DCO-OFDM based WDM VLC. J Lightwave Technol 40:6359–6365

13. Zhang H, Yuan Y, Xu W (2014) PAPR reduction for DCO-OFDM visible light communications via semidefinite relaxation. IEEE Photonics Technol Lett 26(17):1718–1721

14. Hei Y, Liu J, Li W, Xu X, Chen RT (2017) Branch and bound methods based tone injection schemes for PAPR reduction of DCO-OFDM visible light communications. Opt Express 25(2):595–604

15. Noshad M, Brandt-Pearce M (2016) Hadamard-coded modulation for visible light communications. IEEE Trans Commun 64(3):1167–1175

16. Doblado JG, Oria ACO, Baena-Lecuyer V, Lopez P, Perez-Calderon D (2015) Cubic metric reduction for DCO-OFDM visible light communication systems. J Lightwave Technol 33(10):1971–1978

17. Bai J, Li Y, Yi Y, Cheng W, Du H (2017) PAPR reduction based on tone reservation scheme for DCO-OFDM indoor visible light communications. Opt Express 25(20):24630–24638

18. Hei Y, Liu J, Gu H, Li W, Xu X, Chen RT (2017) Improved TKM-TR methods for PAPR reduction of DCO-OFDM visible light communications. Opt Express 25(20):24448–24458

19. Yu Z, Baxley RJ, Zhou GT (2014) Iterative clipping for PAPR reduction in visible light OFDM communications. In: 2014 IEEE military communications conference. IEEE, pp 1681–1686

20. Bandara K, Niroopan P, Chung Y-H (2013) PAPR reduced OFDM visible light communication using exponential nonlinear companding. In: 2013 IEEE international conference on microwaves, communications, antennas and electronic systems (COMCAS 2013). IEEE, pp 1–5

21. Popoola WO, Ghassemlooy Z, Stewart BG (2014) Pilot-assisted PAPR reduction technique for optical OFDM communication systems. J Lightwave Technol 32(7):1374–1382

22. Valluri SP, Kishore V, Vakamulla VM (2020) A new selective mapping scheme for visible light systems. IEEE Access 8:18087–18096

23. Gunturu C, Valluri S (2022) A new complexity reduction scheme in selective mapping-based visible light communication direct current-biased optical orthogonal frequency division multiplexing systems. IET Optoelectron 16(5):207–217

24. Lee WC, Choi JP, Huynh CK (2015) A modified tone injection scheme for PAPR reduction using genetic algorithm. ICT Express 1(2):76–81

25. Lin W-L, Tseng F-S (2021) Theory and applications of active constellation extension. IEEE Access 9:93111–93118

26. Deepa T, Suseela V, Mani V (2022) Performance analysis of novel precoding matrix techniques for optical OFDM-based visible light communication systems. Opt Laser Technol 154:108293

27. Jiang Y (2010) New companding transform for PAPR reduction in OFDM. IEEE Commun Lett 14(4):282–284

28. Eberhart R, Kennedy J (1995) Particle swarm optimization. In: Proceedings of the IEEE international conference on neural networks, vol 4. Citeseer, pp 1942–1948

29. Shi Y, Eberhart R (1998) A modified particle swarm optimizer. In: 1998 IEEE international conference on evolutionary computation proceedings. IEEE world congress on computational intelligence (Cat. No. 98TH8360). IEEE, pp 69–73

30. Kennedy J, Eberhart RC (1997) A discrete binary version of the particle swarm algorithm. In: 1997 IEEE international conference on systems, man, and cybernetics. computational cybernetics and simulation, vol 5. IEEE, pp 4104–4108

31. Wang X, Yao W (2023) A discrete particle swarm optimization algorithm for dynamic scheduling of transmission tasks. Appl Sci 13(7):4353

32. Chen H-W, Liang C-K (2022) Genetic algorithm versus discrete particle swarm optimization algorithm for energy-efficient moving object coverage using mobile sensors. Appl Sci 12(7):3340

33. Cervante L, Xue B, Shang L, Zhang M (2013) A multi-objective feature selection approach based on binary pso and rough set theory. In: Evolutionary computation in combinatorial optimization: 13th European conference, EvoCOP 2013, Vienna, Austria, April 3–5, 2013. Proceedings 13. Springer, pp 25–36

34. Elbeltagi E, Hegazy T, Grierson D (2005) Comparison among five evolutionary-based optimization algorithms. Adv Eng Inform 19(1):43–53

35. Baniabdelghany H, Obermaisser R et al (2021) Reliable task allocation for time-triggered IoT-WSN using discrete particle swarm optimization. IEEE Internet Things J 9(14):11974–11992

36. Huang M, Leung VC, Liu A, Xiong NN (2022) TMA-DPSO: towards efficient multi-task allocation with time constraints for next generation multiple access. IEEE J Sel Areas Commun 40(5):1652–1666

37. Yu Z, Baxley RJ, Zhou GT (2013) Peak-to-average power ratio and illumination-to-communication efficiency considerations in visible light OFDM systems. In: 2013 IEEE international conference on acoustics, speech and signal processing. IEEE, pp 5397–5401